Fluorescence labeling of mitochondria in living cells by the cationic photosensitizer ZnTM2,3PyPz, and the possible roles of redox processes and pseudobase formation in facilitating dye uptake

J. C. Stockert, E. N. Durantini, E. J. Gonzalez Lopez, J. E. Durantini, A. Villanueva & R. W. Horobin

Taylor & Francis
Taylor & Francis Group

Fluorescence labeling of mitochondria in living cells by the cationic photosensitizer ZnTM2,3PyPz, and the possible roles of redox processes and pseudobase formation in facilitating dye uptake

J. C. Stockert[a,b], E. N. Durantini[c], E. J. Gonzalez Lopez[c], J. E. Durantini[d], A. Villanueva[e], and R. W. Horobin[f]

[a]Buenos Aires University, Argentina; [b]Bernardo O'Higgins University, Chile; [c]National University of Río Cuarto, Argentina; [d]National University of Río Cuarto, Argentina; [e]Autonomous University of Madrid, Spain; [f]University of Glasgow, UK

ABSTRACT

The study of labeling selectivity and mechanisms of fluorescent organelle probes in living cells is of continuing interest in biomedical sciences. The tetracationic phthalocyanine-like ZnTM2,3PyPz photosensitizing dye induces a selective violet fluorescence in mitochondria of living HeLa cells under UV excitation that is due to co-localization of the red signal of the dye with NAD(P)H blue autofluorescence. Both red and blue signals co-localize with the green emission of the mitochondria probe, rhodamine 123. Microscopic observation of mitochondria was improved using image processing and analysis methods. High dye concentration and prolonged incubation time were required to achieve optimal mitochondrial labeling. ZnTM2,3PyPz is a highly cationic, hydrophilic dye, which makes ready entry into living cells unlikely. Redox color changes in solutions of the dye indicate that colorless products are formed by reduction. Spectroscopic studies of dye solutions showed that cycles of alkaline titration from pH 7 to 8.5 followed by acidification to pH 7 first lower, then restore the 640 nm absorption peak by approximately 90%, which can be explained by formation of pseudobases. Both reduction and pseudobase formation result in formation of less highly charged and more lipophilic (cell permeant) derivatives in equilibrium with the parent dye. Some of these are predicted to be lipophilic and therefore membrane-permeant; consequently, low concentrations of such species could be responsible for slow uptake and accumulation in mitochondria of living cells. We discuss the wider implications of such phenomena for uptake of hydrophilic fluorescent probes into living cells.

Numerous dyes from different chemical groups are widely used for fluorescence labeling of organelles in living cells (Cañete et al. 2001; Horobin and Kiernan 2002; Stockert et al. 2009; Horobin et al. 2015; Stockert and Blázquez-Castro 2017). Macrocyclic dyes also are currently applied as fluorescent photosensitizers (PS) for photodynamic therapy (PDT) for cancer (Stockert et al. 2004, 2007; Wang et al. 2021).

Like the well-known staining properties of copper-containing phthalocyanine (Pc) dyes (Scott 1980; Juarranz and Stockert 1982; Horobin and Kiernan 2002; Macii et al. 2020; Ali et al. 2022), fluorescent zinc-containing dyes such as ZnPc and its derivatives (Dummin et al. 1997; Villanueva et al. 1999; Maduray et al. 2011; Valli et al. 2019) have been used for PDT. Moreover, like the phthalocyanine-like cuprolinic and cupromeronic blue dyes (Scott 1980; Tas et al. 1983; Juarranz et al. 1987), analogous zinc derivatives have been synthesized (Wöhrle et al. 1985; Asadi et al. 2004),

studied spectroscopically and characterized as useful PS (Dupouy et al. 2004; Tempesti et al. 2008; Spesia et al. 2009). One such compound is zinc(II) tetramethyltetrapyridino[2,3-b:2,3'-g2',3''-l:2'',3'''-q] porphyrazinium (ZnTM2,3PyPz) (Figure 1A), which has a $^1O_2$ quantum yield of $\Phi_\Delta = 0.65$ and a fluorescence quantum yield of $\Phi_F = 0.29$ (Tempesti et al. 2008).
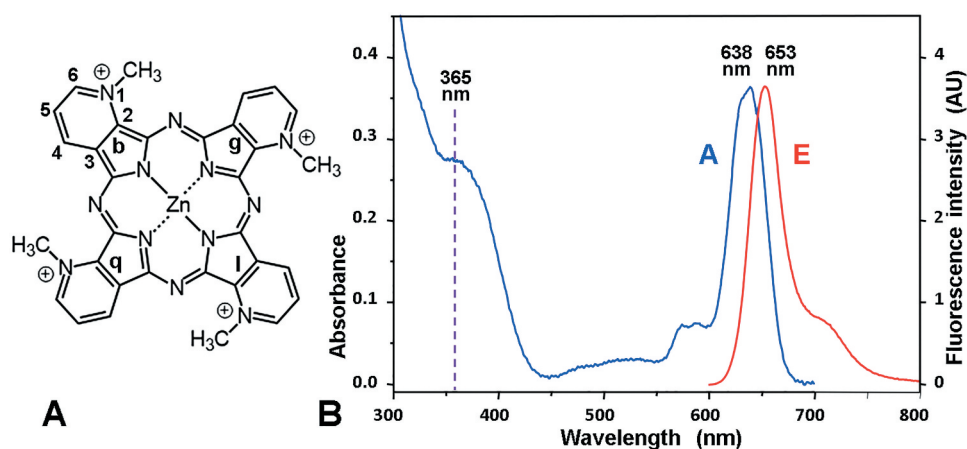
When cultured HeLa cells were incubated with ZnTM2,3PyPz the cells exhibited selective mitochondrial fluorescence, which we describe here. Considering the relation of mitochondria to apoptosis, reactive oxygen species (ROS) and cell signaling (Brillo et al. 2021), the photophysical properties of ZnTM2,3PyPz together with its mitochondrial localization suggest its possible application in PDT for cancer. Consequently, we also consider the question of how these hydrophilic cations enter live cells and accumulate in mitochondria.

Figure 1. A) Chemical structure of ZnTM2,3PyPz with atom numbering of the pyridine ring. B) Absorption (A) and emission (E) spectra of the dye in distilled water (4 μm, λexc = 590 nm), with A and E peaks at 638 nm and 653 nm, respectively, as well as the position of the exciting 365 nm radiation.

Material and methods

Human cervix adenocarcinoma ATCC CCL-2 (American Type Culture Collection, Manassas, VA) HeLa cells, were grown on 22 mm^2 coverslips in 35 mm culture dishes using complete DMEM culture medium containing 10% (v/v) fetal bovine serum, 50 U/ml penicillin, 50 μg/ml streptomycin and 1% (v/v) 0.2 M L-glutamine. Cells were cultured at 37 °C in a humidified atmosphere with 5% CO$_2$ and the medium was changed daily.

The cationic dye, ZnTM2,3PyPz, synthesized according to Tempesti et al. (2008), was a gift from Dr. Tempesti. The dye was dissolved 0.5 mg/ml in phosphate buffered saline (PBS), then diluted with complete DMEM to 50 μg/ml. The mitochondria probe, rhodamine 123 (Rho123) (Green 1990; Horobin and Kiernan 2002), was used to confirm the intracellular localization of the PS. Rho123, 6.5 μg/ml in PBS, was applied for 5 min to cultures incubated previously with the PS followed by washing with PBS. Microscopic observations were made using ultraviolet (UV) (365 nm) and blue (436 nm) exciting light for ZnTM2,3PyPz and Rho123, respectively.

Image processing and analysis were performed using ImageJ v 1.52 software. Convolved images were obtained using the convolve command that used a matrix of 25 points (five columns and five rows, the central point with a value of +25, and the remaining peripheral points with a value of −1) on color 100-dpi JPG images. The convolve filter is adequate for image sharpening and edge detection (Casas et al. 2008; Alvarez et al. 2011; Stockert and Blázquez-Castro 2017). Original violet emission images also were inverted, converted to a binary image and skeletonized (Buño et al. 1998). The red, green and blue channels were isolated by splitting the original violet image. Blue and red images then were compared to those of Rho123.

Aqueous ascorbic acid, 0.5 mg/ml, or 5 mg/ml zinc powder in the presence of 2% (v/v) aqueous acetic acid were used to reduce ZnTM2,3PyPz. The reduced dye then was re-oxidized by exposure to air for 1 h or by addition of 0.5 ml 10% H$_2$O$_2$ in distilled water for 10 min.

UV/visible spectroscopy was performed on a 4 μM dye solution in a 1 cm path length quartz cell at room temperature at different pHs. Aqueous stock solutions, 1.0 x 10^{-3} M, of KOH and HCl were used to adjust the pH to 7, 8.5 and 10, and titrations of the dye in the same cuvette were repeated three times.

Quantitative structure-activity relationships (QSAR) parameters, i.e., charge, log P and conjugated bond number (CBN), were obtained using procedures reported by Horobin et al. (2013, 2015). QSAR models (Horobin et al. 2013, 2015) then were used to predict membrane permeability and organelle localization.

Results

Absorption and emission spectra of ZnTM2,3PyPz are shown in Figure 1B. The high UV absorption appears well suited to excite the dye at 365 nm as occurs with ZnPc and derivatives (Villanueva et al. 1999; Stockert and Blázquez-Castro 2017; Valli et al. 2019). ZnTM2,3PyPz dissolved in distilled water has an extinction coefficient $\varepsilon_{638} = 90,000$ M^{-1} cm^{-1}.

Incubation of HeLa cells with 50 μg/ml ZnTM2,3PyPz for 5 h produced a weak fluorescent signal in mitochondria. Best results were achieved with higher dye concentrations and prolonged

incubation, typically using 0.5 mg/ml in complete DMEM for 20 h (Figure 2A). Under UV excitation, mitochondria exhibited a violet emission due to the co-localization of blue autofluorescence caused by NAD(P)H (Stockert et al. 2009; Stockert and Blázquez-Castro 2017) and the red labeling signal from ZnTM2,3PyPz.

Convolved and binary skeletonized images exhibit the classic thread pattern of mitochondria (Figure 2B, C). Consistent with this, image processing that split the red, green and blue colors from the original violet image revealed complete correspondence between the blue NAD(P)H autofluorescence of mitochondria and the red dye signal (Figure 2D, E). Both blue and red signals also corresponded to the green emission of the selective mitochondria label, Rho123 (Figure 2F).

When subjected to reducing conditions, such as ascorbic acid or zinc powder, dye solutions rapidly become colorless. After removing zinc powder, the blue color was nearly completely recovered by air reoxidation (Figure 3A–C). Likewise, dye reduced by ascorbic acid recovered its blue color after oxidation with H_2O_2.

We measured pH dependent changes in the UV/vis absorption spectrum of ZnTM2,3PyPz. Figure 4 shows that an increase in pH from 7 to 8.5 decreased the absorption of the Q band at 638 nm. Titration of the dye with alkali followed by back-titration with acid largely reproduced the original ZnTM2,3PyPz spectrum with approximately 90% recovery after each cycle (Figure 4, inset). At pH 10, however, the Q band virtually disappeared and there was no recovery (not shown).

Discussion

Aromatic macrocycles such as porphyrins, Pcs- and Pc-like dyes all possess an 18 π electron system that is responsible for their red fluorescence emission. These molecules also all feature high double bond conjugation with CBN values in the 28–48 range. The cationic, zinc-containing phthalocyanine-like dye, ZnTM2,3PyPz (Tempesti et al. 2008), was designed as a PS analogue to cuprolinic blue (Scott 1980); it replaces Cu with Zn to retain the fluorescence of ZnPcs. We observed
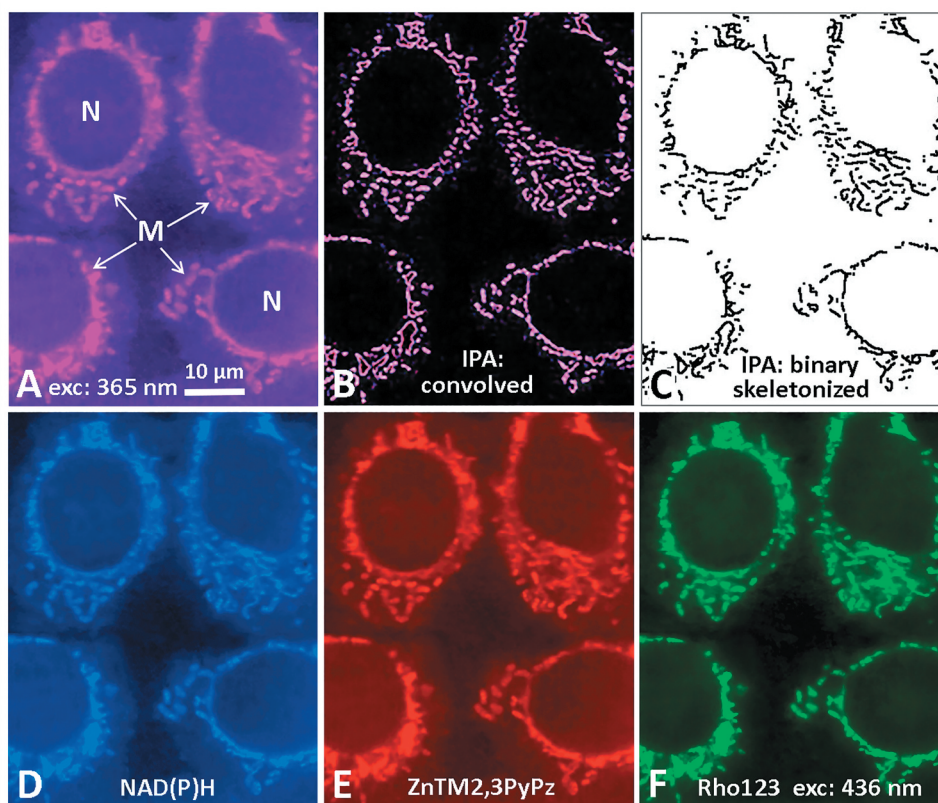
Figure 2. Live HeLa cells incubated with 0.5 mg/ml ZnTm2,3pypz for 20 h. All panels show the same microscopic field. A) Image after using 365 nm excitation; violet labeling of mitochondria (arrows) is due to the merged blue autofluorescence (see panel D) and the red dye signal (see panel E). M, mitochondria; N, nuclei. B) Image after using the convolve filter. C) Image after skeletonizing the binary image. D) Blue autofluorescence due to NAD(P)H. E) Image showing pattern of red emission. F) Green emission of the mitochondrial probe Rho123, resulting from blue excitation, which closely corresponds to the red dye signal seen in panel (E).
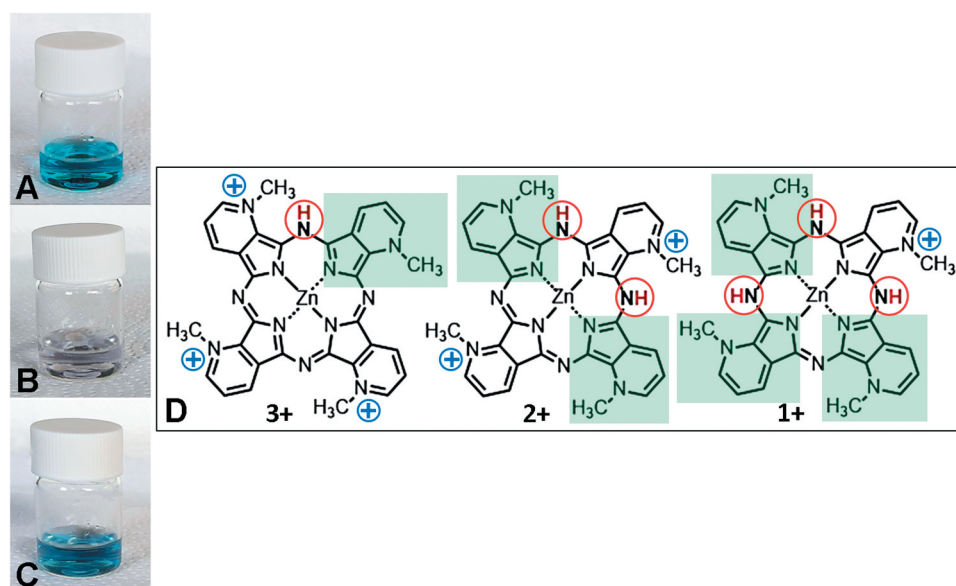
Figure 3. Redox behaviors of ZnTM,3PyPz in aqueous solution. A) Appearance of control solution (5 µg/ml) of dye. B) Effects of adding a reducing agent consisting of 5 mg/ml zincpowder suspended in 2% (v/v) aqueous acetic acid. C) Recoloration due to airreoxidation 1 h after removal of zinc. D) Chemical structures ofpossible reduced products of the dye showing different charged forms (3+, 2+, and 1+), induced by reduction of the macrocycle nitrogen atoms (red circles). This results in formation of lipophilic domains associated with uncharged pyridinemoieties (indicated in green).
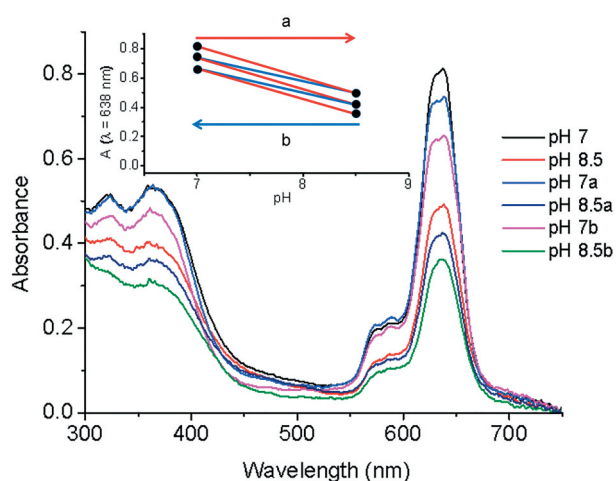

Figure 4. Effect of pH on the UV/visible absorption spectra of ZnTm2,3pypz in aqueous solution: pH 7 and 8.5 indicate a first titration; pH 7a and 8.5a indicate a second titration, pH 7b and 8.5b indicate a third titration. All titrations were repeated three times. Inset: absorbance changes at 638 nm after successive titration cycles: (a) basic titration (pH 7–8.5, red arrow and lines); (b) back acid titration (pH 8.5 to 7, blue arrow and lines).

selective fluorescence labeling only in mitochondria after applying the dye at high concentration and for an extended period of incubation. These requirements for obtaining optimal images are intriguing, because well-known mitochondrial probes, such as the Rho123 that we used, are effective at low concentrations and

short staining times. Possible solutions to this puzzle are discussed below.

According to QSAR numerical modeling (Horobin et al. 2013, 2015), the water soluble and highly charged ZnTM2,3PyPz dye is much too hydrophilic (4+, log P = −10.9) (Table 1) to enter live cells and charge reduction seems to be required to increase the lipophilicity required for membrane permeability. We describe here two mechanisms that could be responsible for such charge reduction.

The first mechanism is dye reduction as occurs for other hydrophilic probes (Stockert et al. 2020). Reduction of ZnTM2,3PyPz yields colorless (Figure 3) and more lipophilic (Table 1) derivatives. These compounds are re-oxidized readily to the cationic form unless kept in an inert atmosphere. If formed near the plasma membrane, however, the reduced and lipophilic dye species could enter live cells rapidly, thus providing a mechanism for dye uptake. Possible reduced forms of ZnTM2,3PyPz are illustrated in Figure 3D; these are similar to the structure proposed for the reduced form of the cobalt-containing phthalocyanine vat dye, indanthrene brilliant blue 4 G (Gurr 1971). Reduction of hydrophilic dyes at the external face of the plasma membrane by NAD(P)H: quinone oxidoreductase 1 (Wondrak 2007) has been proposed as a mechanism for methylene blue and 5-methylphenazinium methyl sulfate staining
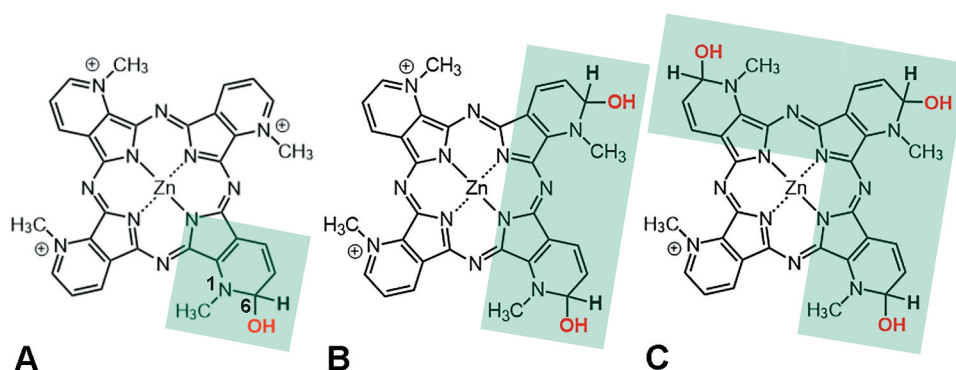
Figure 5. Chemical structures of possible pseudobases derived from ZnTm2,3pypz, with carbinol groups at position 6. Structures of dyes with 3+, 2+, and 1+ charges (A, B, C, respectively) are shown; these result in lipophilic domains associated with uncharged pyridine moieties (indicated in green).

Table 1. QSAR parameters estimated for the tetracationic ZnTM2,3PyPz and for the derived reduced and pseudobase species.

Compound	Charge	Log P	CBN
Parent compound, see Figure 1A	4+	−10.9	48
Reduced species, see Figure 3D	3+	−5.5	46
Species with one pseudobase moiety, see Figure 5A	3+	−6.7	46
Reduced species, see Figure 3D	2+	−0.1	44
Species with two pseudobase moieties, see Figure 5B	2+	−2.5	44
Reduced species, see Figure 3D	1+	5.3	42
Species with three pseudobase moieties, see Figure 5C	1+	1.7	42

(Blázquez-Castro et al. 2009; Stockert et al. 2020). In contact with metals, the color of cuprolinic blue changes reversibly from blue to pink, which appears to be redox behavior (Juarranz et al. 1987). Table 1 shows that a membrane-permeant species requires reduction of more than a single nitrogen substituent; the low probability of this could underlie the need for high dye concentrations and long incubation times.

The second possible mechanism depends on the fact that whereas some protonated basic dyes are in equilibrium with their free bases, certain *N*-quaternary salts form pseudobases (Bunting and Norris 1977; Bunting 1980). Because the resulting carbinols are more lipophilic than the parent salt, this could constitute another mechanism for dye uptake. Although equilibria involving protons are extremely fast, pseudobase-cation interconversion rates vary and some are very slow. This may explain, for example, why ethidium bromide, whose cationic character is due to a quaternary salt, although possessing a moderately lipophilic pseudobase, nevertheless enters live cells slowly and in a concentration-dependent manner (Horobin et al. 2006). To explore the possible role of pseudobase formation on dye permeability, we estimated log P and CBN (Table 1). Our findings indicate that conversion of a single pyridinium moiety

to a pseudobase causes a substantial decrease in hydrophilicity that is equivalent to adding at least four methyl groups to the molecule. Figure 4 shows pH dependent changes in the UV/visible spectrum that could be due to this phenomenon. The chemical structures of the possible carbinol pseudobases are shown in Figure 5.

Table 1 and the QSAR models (Horobin et al. 2013, 2015) suggest that the 1+ species, a lipophilic cation, would be membrane-permeant and would accumulate in mitochondria. It is unlikely, however, that such a species, whose formation requires conversion of three of the four pyridinium moieties on each molecule to pseudobases (Figure 5), would constitute more than a small proportion of the dye present. This might also be a solution to the puzzle of why mitochondrial staining was seen only at high dye concentration and a long incubation period. There also is a way that the 2+ species, which might be present in a greater concentration, might enter the cell. If the two quaternary N+ were adjacent, then the resulting molecule would be asymmetric and amphiphilic (Figure 5) and the lipophilic domain could insert into the plasma membrane. Owing to the embedding of the formal N+ site within the heterocycle and to the *N*-Me substituent, there is no

local domain that is sufficiently hydrophilic to prevent such a molecule from passing through the membrane, which would allow the dye to enter the cell by a flip-flop process. Because selective mitochondrial accumulation requires the presence of lipophilic cations, however, formation of a 1+ species would again constitute a rate controlling step. According to the accepted view (Bunting and Norris 1977; Bunting 1980), the insertion of OH is expected to take place at position C6 of the pyridinium ring.

The reported rates of formation of dye pseudobases vary widely, with half-reaction times falling in the range of seconds to hours. Steric obstruction, such as in the large dye molecules discussed here, is one factor that causes slow rates We observed that the absorbance of ZnTM2,3PyPz decreased at basic pH and that the process was largely reversed upon returning the solution to neutral pH; this supports the concept of pseudobase formation. The small loss of reversibility could be due to a side reaction that converts pyridinium pseudobases to dihydro derivatives (Moracci et al. 1976; Ali et al. 2022), which, however, with macrocycles only becomes significant at pH 11.

Although we discuss here the puzzling permeability behavior of a single dye, ZnTM2,3PyPz, we wish to emphasize that the role of membrane-permeant reduced species and pseudobases in facilitating cell entry of hydrophilic probes and PS could be a more widespread phenomenon. In particular, these processes could be involved in the uptake of other cationic CuPc, ZnPc and Pc-like dyes into living cells (Dupouy et al. 2004; Spesia et al. 2009; Valli et al. 2019; Ali et al. 2022) and may also be involved in the uptake of pyridinium-containing fluorescent probes. There are numerous compounds of this kind, including styryl probes such as 4-Di-2-ASP, DASPEI and DASPI. These three have been applied extensively as mitochondria-localizing probes; however, they differ markedly from the usual cationic mitochondrial probes, such as Rho, because these three are hydrophilic, not lipophilic. Estimated log P values for these three dyes are −0.4, −0.9 and −0.9 respectively.

Two non-exclusive mechanisms, i.e., formation of reduced or pseudobase lipophilic species, may underlie the puzzling permeability behavior of ZnTM2,3PyPz. Because experimental evidence indicates that both processes might be possible with ZnTM2,3PyPz, the puzzle has not been resolved completely. Our findings do indicate that more attention should be paid to how certain hydrophilic fluorescent probes succeed in entering living cells and also that possible formation of reduced or pseudobase species should always be considered.

Disclosure statement

The authors declare no conflict of interest.

References

Ali S, Dapson RW, Horobin RW, Kiernan JA, Kazlauciunas A. 2022. At least four distinct blue cationic phthalocyanine dyes sold as "alcian blue" raises the question: what is alcian blue? Biotech Histochem. 97:11–20. doi:10.1080/10520295.2021.2018497.

Alvarez M, Villanueva A, Acedo P, Cañete M, Stockert JC. 2011. Cell death causes relocalization of photosensitizing fluorescent probes. Acta Histochem. 113:363–368. doi:10.1016/j.acthis.2010.01.008.

Asadi M, Elham Safaei E, Bijan Ranjbar B, Hasani L. 2004. Thermodynamic and spectroscopic study on the binding of cationic Zn(II) and Co(II) tetrapyridino porphyrazines to calf thymus DNA: the role of the central metal in binding parameters. New J Chem. 28:1227–1234. doi:10.1039/b404068f.

Blázquez-Castro A, Stockert JC, Sanz-Rodríguez F, Zamarrón A, Juarranz A. 2009. Differential photodynamic response of cultured cells to methylene blue and toluidine blue: role of dark redox processes. Photochem Photobiol Sci. 8:371–376. doi:10.1039/b818585a.

Brillo V, Chieregato L, Leanza L, Muccioli S, Costa R. 2021. Mitochondrial dynamics, ROS, and cell signaling: a blended overview. Life. 11:332. doi:10.3390/life11040332.

Buño I, Juarranz A, Cañete M, Villanueva A, Gosálvez J, Stockert JC. 1998. Image processing and analysis of fluorescent labelled cytoskeleton. Micron. 29:445–449. doi:10.1016/S0968-4328(98)00023-7.

Bunting JW, Norris DJ. 1977. Rates and equilibria for hydroxide ion addition to quinolinium and isoquinolinium cations. J Am Chem Soc. 99:1189–1196. doi:10.1021/ja00446a034.

Bunting JW. 1980. Heterocyclic pseudobases. Adv Heterocyclic Chem. 25:1–82.

Cañete M, Juarranz A, López-Nieva P, Alonso-Torcal C, Villanueva A, Stockert JC. 2001. Fixation and permanent mounting of fluorescent probes after vital labeling of cultured cells. Acta Histochem. 103:117–126. doi:10.1078/0065-1281-00594.

Casas A, Sanz-Rodríguez F, Di Venosa G, Rodriguez L, Mamone L, Blázquez A, Jaén P, Batlle A, Stockert JC, Juarranz A. 2008. Disorganisation of cytoskeleton in cells resistant to photodynamic treatment with decreased metastatic phenotype. Cancer Lett. 270:56–65. doi:10.1016/j.canlet.2008.04.029.

Dummin H, Cernay T, Zimmermann HW. 1997. Selective photosensitization of mitochondria in HeLa cells by cationic Zn(II)phthalocyanines with lipophilic side-chains. J Photochem Photobiol B. 37:219–229. doi:10.1016/s1011-1344(96)07416-7.

Dupouy EA, Lazzeri D, Durantini EM. 2004. Photodynamic activity of cationic and non-charged Zn(II) tetrapyridinoporphyrazine derivatives: biological consequences in human erythrocytes and *Escherichia coli*. Photochem Photobiol Sci. 3:992–998. doi:10.1039/b407848a.

Green FJ. 1990. The Sigma-Aldrich handbook of stains, dyes and indicators. Aldrich Chemical Cop. Inc.: Milwaukee, WI; p. 626.

Gurr E. 1971. Synthetic dyes in biology, medicine and chemistry. Academic Press: London, New York; p. 706.

Horobin RW, Kiernan JA. 2002. Conn's biological stains. A handbook of dyes, stains and fluorochromes for use in biology and medicine. 10th ed. Bios Scientific Publishers: Oxford; p. 240, 379.

Horobin RW, Stockert JC, Rashid-Doubell F. 2006. Fluorescent cationic probes for nuclei of living cells: why are they selective? A quantitative structure–activity relations analysis. Histochem Cell Biol. 126:165–175. doi:10.1007/s00418-006-0156-7.

Horobin RW, Stockert JC, Rashid-Doubell F. 2013. Uptake and localisation of small-molecule fluorescent probes in living cells: a critical appraisal of QSAR models and a case study concerning probes for DNA and RNA. Histochem Cell Biol. 139:623–637. doi:10.1007/s00418-013-1090-0.

Horobin RW, Stockert JC, Rashid-Doubell F. 2015. Uptake and localization mechanisms of fluorescent and colored lipid probes. Part 2. QSAR models that predict localization of fluorescent probes used to identify ("specifically stain") various biomembranes and membranous organelles. Biotech Histochem. 90:241–254. doi:10.3109/10520295.2015.1005129.

Juarranz A, Stockert JC. 1982. Monastral fast blue. Cytochemical properties of a reaction product from alcian blue stained chromatin. Acta Histochem. 70:130–134. doi:10.1016/S0065-1281(82)80106-2.

Juarranz A, Ferrer JM, Tato A, Cañete M, Stockert JC. 1987. Metachromatic staining and electron dense reaction of glycosaminoglycans by means of cuprolinic blue. Histochem J. 19:1–6. doi:10.1007/BF01675286.

Macii F, Arnaiz CP, Arrico L, Busto N, Garcia B, Biver T. 2020. Alcian blue pyridine variant interaction with DNA and RNA polynucleotides and G-quadruplexes: changes in the binding features for different biosubstrates. J Inorg Biochem. 212:111199. doi:10.1016/j.jinorgbio.2020.111199.

Maduray K, Karsten A, Odhav B, Nyokong T. 2011. In vitro toxicity testing of zinc tetrasulfophthalocyanines in fibroblast and keratinocyte cells for the treatment of melanoma cancer by photodynamic therapy. J Photochem Photobiol B. 103:98–104. doi:10.1016/j.jphotobiol.2011.01.020.

Moracci FM, Casini A, Liberatore F, Carelli V. 1976. Dihydropyridines and pyridones from 3-cyano-1-methylpyridinium iodide in aqueous NaOH. Tetrahedron Lett. 17:3723–3724. doi:10.1016/s0040-4039(00)93092-2.

Scott JE. 1980. The molecular biology of histochemical staining by cationic phthalocyanine dyes: the design of replacements for alcian blue. J Microsc. 119:373–381. doi:10.1111/j.1365-2818.1980.tb04108.x.

Spesia MB, Caminos DA, Pons P, Durantini EN. 2009. Mechanistic insight of the photodynamic inactivation of *Escherichia coli* by a tetracationic zinc(II) phthalocyanine derivative. Photodiagn Photodyn Ther. 6:52–61. doi:10.1016/j.pdpdt.2009.01.003.

Stockert JC, Juarranz A, Villanueva A, Nonell S, Horobin RW, Soltermann AT, Durantini EN, Rivarola V, Colombo LL, Espada J, Cañete M. 2004. Photodynamic therapy: selective uptake of photosensitizing drugs into tumor cells. Curr Top Pharmacol. 8:185–217.

Stockert JC, Cañete M, Juarranz A, Villanueva A, Horobin RW, Borrell JI, Teixidó J, Nonell S. 2007. Porphycenes: facts and prospects in photodynamic therapy of cancer. Curr Med Chem. 14:997–1026. doi:10.2174/092986707780362934.

Stockert JC, Villanueva A, Cristóbal J, Cañete M. 2009. Improving images of fluorescent cell labeling by background signal subtraction. Biotech Histochem. 84:63–68. doi:10.1080/10520290902804357.

Stockert JC, Blázquez-Castro A. 2017. Fluorescence microscopy in life sciences. Bentham Science Publishers: Sharjah, U.A.E. doi:10.2174/978168108.51801170101.

Stockert JC, Carou MC, Casas AG, García Vior MC, Ezquerra Riega SD, Blanco MM, Espada J, Blázquez-Castro A, Horobin RW, Lombardo DM. 2020. Fluorescent redox-dependent labeling of lipid droplets in cultured cells by reduced phenazine methosulfate. Heliyon. 6: e04182. doi:10.1016/j.heliyon.2020.e04182.

Tas J, Mendelson D, van Noorden CJF, Noorden CJF. 1983. Cuprolinic blue: a specific dye for single-stranded RNA in the presence of magnesium chloride. I. Fundamental aspects. Histochem J. 15:801–814. doi:10.1007/BF01003343.

Tempesti TC, Stockert JC, Durantini EN. 2008. Photosensitization ability of a water-soluble zinc(II) tetramethyltetrapyridinoporphyrazinium salt in aqueous solution and biomimetic reverse micelles medium. J Phys Chem B. 112:15701–15707. doi:10.1021/jp808094q.

Valli F, García Vior MC, Roguin LP, Marino J. 2019. Oxidative stress generated by irradiation of a zinc(II) phthalocyanine induces a dual apoptotic and necrotic response in melanoma cells. Apoptosis. 24:119–134. doi:10.1007/s10495-018-01512-w.

Villanueva A, Domínguez V, Polo S, Vendrell VD, Sanz C, Cañete M, Juarranz A, Stockert JC. 1999. Photokilling mechanisms induced by zinc(II)-phthalocyanine on cultured tumor cells. Oncology Res. 11:447–453.

Wang Z, Peng H, Shi W, Gan L, Zhong L, He J, Xie L, Wu P, Zhao Y, Deng Z, Tang H, Huang Y. 2021. Application of photodynamic therapy in cancer: challenges and advancements. Biocell. 45:489–500. doi:10.32604/biocell.2021.014439.

Wöhrle D, Gitzel J, Okura I, Aono S. 1985. Photoredox properties of tetra-2,3-pyridinoporphyrazines (29H,31H-tetrapyrido[2,3-b: 2′, 3′-g : 2″,3″-l:2‴,3‴-q]porphyrazine). J Chem Soc Perk Trans. 2:1171–1178. doi:10.1039/P29850001171.

Wondrak GT. 2007. NQO1-Activated phenothiazinium redox cyclers for the targeted bioreductive induction of cancer cell apoptosis. Free Rad Biol Med. 43:178–190. doi:10.1016/j.freeradbiomed.2007.03.035.